Article ID: 1006-8775(2001) 02-0199-10

SST THERMAL FORCING – A DISCUSSION ON THE MECHANISM OF ATMOSPHERIC LOW-FREQUENCY OSCILLATION

ZHANG Ren (**张　韧**)[1], YU Zhi-hao (**余志豪**)[2], JIANG Quan-rong (**蒋全荣**)[2], JIANG Guo-rong (**蒋国荣**)[1]

(1 *Meteorological Institute, China PLA University of Science and Technology, Nanjing*, 211101 *China*; 2. *Department of Atmospheric Sciences*, *Nanjing University*, *Nanjing* 210093 *China*)

ABSTRACT: Dynamic and numerical methods are used to discuss the atmospheric response to SST thermal forcing. The results show that for planetary scale systems, the standing SST thermal forcing can quickly excite a stable atmospheric equilibrium state response, which is characterized by obvious large-scale teleconnection oscillation in east-west and south-north directions. For synoptic scale systems, the SST thermal forcing mainly excites the atmospheric low-frequency oscillation. Some basic relation and dynamic processes between SST thermal forcing and atmospheric response pattern are revealed and some new viewpoints are presented.

Key words: SST fields; thermal forcing; oscillation; low-frequency fluctuation

CLC number: P434.1 **Document code:** A

1 INTRODUCTION

In the air-sea system, the effect of ocean on the atmosphere is mainly shown as thermal forcing. Subject to the condition, there is a large-scale out-of-phase teleconnection in the tropical atmosphere. More than half a century ago, Walker discovered the Southern Oscillation (SO). Since the 1980's, pressure fields that were similar to the phenomenon of negative east-west correlation in the SO was found to be present in the middle- and lower-latitude regions of the Northern Hemisphere, which was called Northern Oscillation (NO)[1]. As shown in some research, atmospheric forcing of external sources, especially the anomalies of tropical SST, can have very significant tele-response. The remote response of global atmosphere to SST anomalies forms a stable teleconnection pattern[2]. The importance of the oceanic thermal effect on the oscillation in the tropics is also displayed in close association between various teleconnection patterns and SST distribution ones, such as El Niño and ENSO. Although there is reported significant atmospheric response to external source forcing, not many attempts have been made to discuss the principal characteristics[3]. In many of the study and experiments, focus is on dealing with the response of atmospheric circulation to local SST anomalies. Examples include the discovery of anomalous warming of SST in the equatorial eastern Pacific being favorable for the appearance of PNA teleconnection patterns[2, 3], close linkage between the Pacific-Japan (P–J) oscillation (wavetrain) and the convective activity in the western Pacific warm pool[4], and similar anomalies in the atmospheric response to positive SST anomaly in the Kuroshio area. In view of it, the current work intends to incorporate three typical SST distribution patterns fully, including a normal configuration of being colder in the east

Received date: 2000-03-06; **revised date:** 2001-08-21

Foundation item: Foundation for Backbone Teachers in Higher Colleges of Education Ministry; Natural Science Foundation of China (49975012)

Biography: ZHANG Ren (1963 –), male, native from Emei County of Sichuan Province, professor, Ph.D, mainly undertaking the study on tropical and oceanic meteorology.

than in the west and two anomalous processes of El Niño / La Niña and to discuss and compare how the atmosphere responses to the SST-structured forcing. In addition, the oceanic thermal effect on the tropical low-frequency oscillation is shown as importantly. Being an external forcing, SST is an easy mechanism to excite low-frequency oscillation[3]. The low-frequency oscillation in the tropical region is a topic that has been discussed in depth systematically, though with focus more on the aspect of low-frequency propagation and dissipation mechanisms[1, 3]. Relatively speaking, fewer attempts have been made to study the corresponding relation between the heat source forcing and the structure of low-frequency oscillation and their temporal and spatial features. It is on this aspect that this paper has been working.

2 DYNAMIC MODEL

This section involves itself with a discussion of distribution patterns of varying SST over the tropical Pacific Ocean and atmospheric response modes as possible consequences of the anomalous SST fields. As both temporal and spatial scales are quite large in the system at the time, an approximate atmospheric forcing and dissipating shallow-water model on the equatorial β-plane, which includes the oceanic thermal effect, is used as follows:

$$\begin{cases} \dfrac{\partial u}{\partial t}+u\dfrac{\partial u}{\partial x}+v\dfrac{\partial u}{\partial y}-fv+g\dfrac{\partial h}{\partial x}=-Au \\ \dfrac{\partial v}{\partial t}+u\dfrac{\partial v}{\partial x}+v\dfrac{\partial v}{\partial y}+fu+g\dfrac{\partial h}{\partial y}=-Av \\ \dfrac{\partial h}{\partial t}+u\dfrac{\partial h}{\partial x}+v\dfrac{\partial h}{\partial y}+h\dfrac{\partial u}{\partial x}+h\dfrac{\partial v}{\partial y}=-Bh-Q_S \end{cases} \tag{1}$$

For large-scale atmospheric and oceanic motion in the tropics, the quasi-geostrophic filtering approximation[6] is used. From Eq.(1), a set of barotropic vorticity and thermodynamic equations is obtained:

$$\begin{cases} \dfrac{\partial}{\partial t}\nabla^2 y+J(y,\nabla^2 y)+b\dfrac{\partial y}{\partial x}=-A\nabla^2 y \\ \dfrac{\partial h}{\partial t}+J(y,h)=-Bh-Q_S \end{cases} \tag{2}$$

in which $\nabla^2 y=\dfrac{\partial^2 y}{\partial x^2}+\dfrac{\partial^2 y}{\partial y^2}$, $J(a,b)=\dfrac{\partial a}{\partial x}\dfrac{\partial b}{\partial y}-\dfrac{\partial a}{\partial y}\dfrac{\partial b}{\partial x}$ are relatively the 2-dimensional Hermitian operator and Jacobian operator, h is the height of atmospheric geopotential, and A, B are relatively the atmospheric Rayleigh frictional coefficient and Newton cooling coefficient. The thermal effect imposed by the ocean on the atmosphere can be expressed as $Q_s=aH_s$, in which H_s is the thickness of oceanic thermocline and a is the parameter of ratio. With scaling, we know that $(x,y)\sim L_0(x',y'), t\sim T_0 t'\sim \dfrac{L_0}{U_0}t', y\sim U_0 L_0 y', h\sim H_0 h', H_s\sim H_{s0}H_s'$, in which H_{s0} is the characteristic thickness of oceanic thermocline. Substituting the above conversion, we get a dimensionless equation set of

$$\begin{cases} \dfrac{\partial}{\partial t}\nabla^2 y + J(y,\nabla^2 y) + C_0\dfrac{\partial y}{\partial x} = -D_0\nabla^2 y \\ \dfrac{\partial h}{\partial t} + J(y,h) = -F_0 h - G_0 H_s \end{cases} \tag{3}$$

where $C_0 = b\dfrac{L_0^{\,2}}{U_0}, D_0 = A\dfrac{L_0}{U_0}, F_0 = B\dfrac{L_0}{U_0}, G_0 = a\dfrac{L_0 H_{S0}}{U_0 H_0}$.

For brevity, dimensionless variables in the equation have eliminated the " ′ " sign.

In our discussion of the response of tropical atmosphere to the thermal forcing in the ocean, the emphasis is on the role of the SST field in the tropical eastern and western Pacific Ocean. For the convenience of discussion, the domain of topic will be confined to the regions of South Asia and tropics / subtropics in the Pacific within 30° on both side of the equator. The model is bounded by $D = \{x: 0 \le x \le \pi, y: -\pi/6 \le y \le \pi/6\}$, in which the left boundary $x = 0$ is approximately located at 60°E on the western coast of the Indian Ocean and the right one $x = \pi$ is roughly at 120°W on the eastern coast of the Pacific Ocean; $x1 = \{0, p/2\}$ is the monsoon region in South Asia, $x2 = \{p/2, p\}$ is the trade wind area in the Pacific and $y = \{-p/6, p/6\}$. They generally contain all major thermal regions in the underlying oceanic surface that affects the tropical atmosphere. For the regions of interest presented above, the characteristic function of the Laplace operator is used as basis function. As the study is about the dynamics, the higher-order truncation of spectrum is adopted, in which only the following three complete orthogonal cuts are used:

$$f_1(x,y) = \frac{\sqrt{2}}{\pi}\sin(6y), \qquad f_2(x,y) = \frac{2}{\pi}\cos(3y)\sin(x), \qquad f_3(x,y) = \frac{2}{\pi}\cos(6y)\cos(x)$$

Then, w, h and H_s are expanded respectively as basis function:

$$y(x,y,t) = y_1(t) f_1(x,y) + y_2(t) f_2(x,y) + y_3(t) f_3(x,y)$$

$$h(x,y,t) = h_1(t) f_1(x,y) + h_2(t) f_2(x,y) + h_3(t) f_3(x,y)$$

$$H_s(x,y,t) = H_{s1}(t) f_1(x,y) + H_{s2}(t) f_2(x,y) + H_{s3}(t) f_3(x,y)$$

The family of basis function usually falls into basic patterns of SST field in tropical Pacific region of the Northern Hemisphere. The expressions above are substituted into the equation set Eq.(3) for reduction of this partial difference equation into an ordinary differential system. It is then multiplied respectively by f_1, f_2, f_3 before regional integration along $x \in [0,\pi]$ and $y \in [-\pi/6, \pi/6]$ for six first-order equation set of ordinary differential control system:

$$\begin{cases} \dfrac{dy_1}{dt} = -\dfrac{1}{37.699}[-14.445 y_2 y_3 + 37.699 D_0 y_1] \\ \dfrac{dy_2}{dt} = -\dfrac{1}{10.472}[0.535 y_1 y_3 + 0.141 C_0 y_3 + 10.472 D_0 y_2] \\ \dfrac{dy_3}{dt} = -\dfrac{1}{38.746}[13.91 y_1 y_2 - 0.141 C_0 y_2 + 38.746 D_0 y_3] \\ \dfrac{dh_1}{dt} = \dfrac{0.535}{0.333}[y_2 h_3 - y_3 h_2] - F_0 h_1 - G_0 H_{s1} \\ \dfrac{dh_2}{dt} = -\dfrac{0.535}{0.333}[y_1 h_3 - y_3 h_1] - F_0 h_2 - G_0 H_{s2} \\ \dfrac{dh_3}{dt} = \dfrac{0.535}{0.333}[y_1 h_2 - y_2 h_1] - F_0 h_3 - G_0 H_{s3} \end{cases} \tag{4}$$

3 EQUILIBRIUM STATE AND ANALYSIS OF ITS STABILITY

With regard to the dynamics in a quasi-stationary condition of the above non-linear ordinary differential system, discussions can be held from the point of the equilibrium state. An equation set of equilibrium state corresponding to Eq.(4) is written as:

$$\begin{cases} -14.445y_2y_3 + 37.699D_0y_1 = 0 \\ 0.535y_1y_3 + 0.141C_0y_3 + 10.472D_0y_2 = 0 \\ 13.91y_1y_2 - 0.141C_0y_2 + 38.746D_0y_3 = 0 \\ 0.535(y_2h_3 - y_3h_2) - 0.333(F_0h_1 + G_0H_{s1}) = 0 \\ 0.535(y_1h_3 - y_3h_1) + 0.333(F_0h_2 + G_0H_{s2}) = 0 \\ 0.535(y_1h_2 - y_2h_1) - 0.333(F_0h_3 + G_0H_{s3}) = 0 \end{cases} \tag{5}$$

For a given parameter value, the solution of an equilibrium state can be sought numerically: In $\overline{y}_1, \overline{y}_2, \overline{y}_3, \overline{h}_1, \overline{h}_2, \overline{h}_3$, values are so taken that $U_0 \sim 10\,\mathrm{m}$, $A = 1.16\times10^{-7}$ /s, $B = 2.32\times10^{-7}$ /s, $a = 1.0\times10^{-2}$ /s, $H_{s0} \sim 40\,\mathrm{m}$, $H_0 \sim 1.0\times10^3\,\mathrm{m}$, and $b = 2.25\times10^{-11}$ /sm (about 10°N). Based on basic observed facts and real weather characteristics, the model's SST distribution patterns are shown as the following, which are displayed in the form of thermocline anomaly:

(1) For $H_{s1} = 0.5, H_{s2} = 0.3, H_{s3} = 1.2$, a general picture of normal anomaly distribution is presented in which the South China Sea and tropical western Pacific are a warm SST region while the equatorial eastern Pacific is a cold water zone, according to what is taken for the basis function (Fig.1).

(2) For $H_{s1} = 0.5, H_{s2} = -0.3, H_{s3} = 1.2$, a general picture of La Niña distribution is presented in which the warm pool in the west Pacific is weakening in the anomaly and retreating to the west while the cool pool in the equatorial west Pacific intensifies anomalously and expands westward (Fig.2).

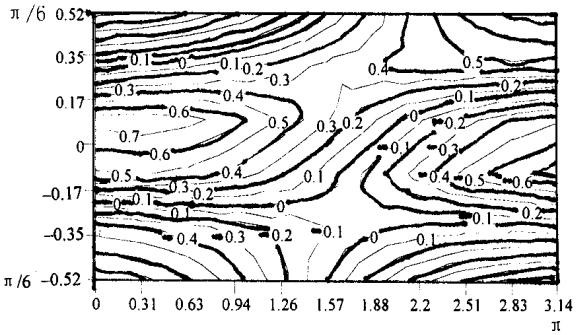

Fig.1 Pattern I of the SST distribution in the Pacific.

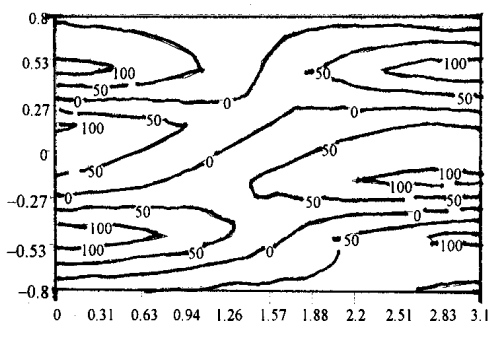

Fig.2 Pattern II of the SST distribution in the Pacific.

(3) For $H_{s1} = 0.5, H_{s2} = 0.3, H_{s3} = -1.2$, a general picture of El Niño distribution is presented in which the west Pacific is cooler in the anomaly and east Pacific intensifies SST is warming anomalously (Fig.3).

When the horizontal scale takes $L_0 \sim 10^7\,\mathrm{m}$, we find that the atmospheric system is of planetary scale. In the meantime, the initial field is set by assuming that $[y_1, y_2, y_3] = 1.0, -0.5, -1.0_0$, $[h_1, h_2, h_3]_0 = [1.0, -0.5, -1.5]$. Such configuration succeeds in depicting the distribution of tropical and subtropical regions of the Pacific Ocean and weather situation in East Asia in the summertime.

With different types of SST distribution corresponding to the above initial condition, an equilibrium state in which atmospheric geopotential responses to the thermal forcing is derived separately.

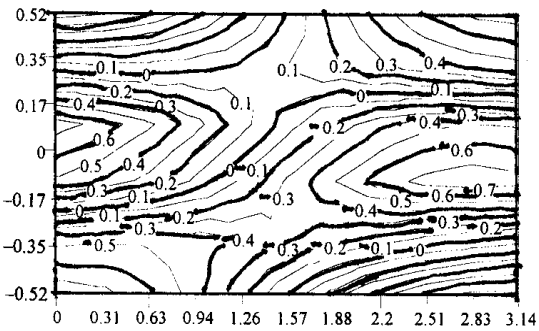

Fig.3 Pattern III of the SST distribution in the Pacific.

① In response to the thermal forcing of Type I SST, the atmospheric geopotential has the only equilibrium state of $[\bar{h}_1, \bar{h}_2, \bar{h}_3] = [-86.2, -51.7, -207]$. The same results can be obtained by taking numerical integration of Eq.(4). When the integration steps into its 40th day, disturbances in the atmospheric geopotential tend to be stationary with the value consistent with the above equilibrium state. On the other hand, disturbances in the atmospheric wind field tend to be in a zero equilibrium state (figure omitted).

② In response to the thermal forcing of Type II SST, the atmospheric geopotential also adapts quickly towards the equilibrium state: $[\bar{h}_1, \bar{h}_2, \bar{h}_3] = [-86.2, 51.7, -207]$.

③In response to the thermal forcing of Type III SST, the atmospheric geopotential also adapts quickly towards the equilibrium state: $[\bar{h}_1, \bar{h}_2, \bar{h}_3] = [-86.2, -51.7, 207]$.

In our discussion of the stability of the solution to the equilibrium state above, the method of perturbation is used to linearlize the non-linear ordinary differential equation set:

We set $y_1 = \bar{y}_1 + y_1'$, $y_2 = \bar{y}_2 + y_2'$, $y_3 = \bar{y}_3 + y_3'$, $h_1 = \bar{h}_1 + h_1'$, $h_2 = \bar{h}_2 + h_2'$, $h_3 = \bar{h}_3 + h_3'$, in which $y_1', y_2', y_3', h_1', h_2', h_3'$ is the quantity of disturbance. The stability of the non-linear system can be described by a linear ordinary differential system, which is based on the solution to its equilibrium state. The perturbation is substituted into Eq.(4) before subtracting the equation for equilibrium solutions so that a linearized perturbation equation set is determined that is close to the point of equilibrium and shown in the form of matrix:

$$\frac{\mathrm{d}X}{\mathrm{d}t} = AX \tag{6}$$

where $X = \begin{pmatrix} y_1 \\ y_2 \\ y_3 \\ h_1 \\ h_2 \\ h_3 \end{pmatrix}$ $A = \begin{bmatrix} -D_0 & a\bar{y}_3 & a\bar{y}_2 & 0 & 0 & 0 \\ -b\bar{y}_3 & -D_0 & -(b\bar{y}_1 + cC_0) & 0 & 0 & 0 \\ -d\bar{y}_2 & (eC_0 - d\bar{y}_1) & -D_0 & 0 & 0 & 0 \\ 0 & k\bar{h}_3 & -k\bar{h}_2 & -F_0 & -k\bar{y}_3 & k\bar{y}_2 \\ -k\bar{h}_3 & 0 & k\bar{h}_1 & k\bar{y}_3 & -F_0 & -k\bar{y}_1 \\ k\bar{h}_2 & -k\bar{h}_1 & 0 & -k\bar{y}_2 & k\bar{y}_1 & -F_0 \end{bmatrix}$

in which $\bar{y}_1, \bar{y}_2, \bar{y}_3, \bar{h}_1, \bar{h}_2, \bar{h}_3$ is the equilibrium solution derived. For the sake of brevity, the rest of the perturbation variables in the equation have dropped the sign " ′ ". Specifically, $a = 0.383$, $b = 0.051$, $c = 0.013$, $d = 0.359$, $e = 0.004$, $k = 1.607$.

According to the stability theory of Lyapunov, if the real part of all eigenvalues in the coefficient matrix A is smaller than zero for all solutions of equilibrium states, the equilibrium state for Eq.(4) is stable; if the real part is larger than zero for more than 1 eigenvalue, the equilibrium state has an unstable solution in the system. Substituting the solution to the equilibrium state into the matrix A for determination of its characteristic root l, we know that $R(l_{\max}) = -0.116 < 0$ (with

the maximum characteristic root less than zero). The result shows that the equilibrium state, which is corresponding to the atmospheric geopotential response of the above three types of sea surface temperature, is stable.

4 GEOPOTENTIAL FIELD CORRESPONDING TO EQUILIBRIUM STATE AT PLANETARY SCALE

(1) By way of basis-function transformation, the atmospheric geopotential of the equilibrium state is shown in Fig.4, for Point ① in Section 3 of the current paper. It is noted that the equatorial eastern Pacific region is positive and the tropical western Pacific and South China Sea region is negative, in the model anomaly. Things are just the opposite in the subtropical region (20°N ~ 30°N). The anomalous response is negative (positive) in the eastern Pacific Ocean (western East Asia monsoon region), displaying a significant pattern of east-west oscillation.

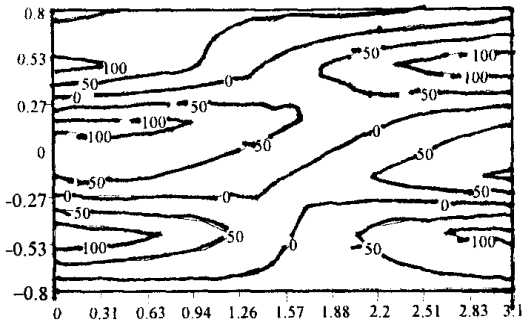

Fig.4 Atmospheric equilibrium state responding to Pattern I of SST

(2) For Point ② in Section 3, the atmospheric geopotential of the equilibrium state is shown in Fig.5, being similar to Fig.4 in general situation. One should note, however, that the amplitude and domain of the positive anomaly is substantially strengthened and westward-enlarged for the geopotential response in the equatorial east Pacific and those of the negative anomaly is reduced and westward-shrunk in the tropical western Pacific. At the time, a significant positive anomalous response in the atmospheric geopotential field appears in the western part of the subtropics (20°N ~ 30°N). There are not only significant east-west oscillations but also strong north-south negative correlation at both east and west boundaries of the model. It shows that the mode of oscillation is strong in the north-south direction in addition to significant east-west oscillation response during the La Niña period. As significant positive response is over the subtropical region of East Asia of the model, we confer that the SST pattern over the La Niña period is favorable for the strengthening and northward progression of the west-Pacific subtropical high in the summer or the steered northward stay of the high over an extended period.

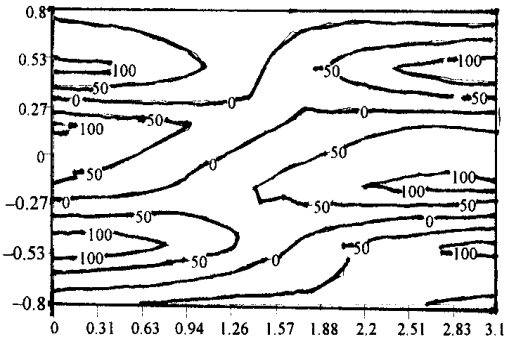

Fig.5 Same as Fig.4 but for Pattern II.

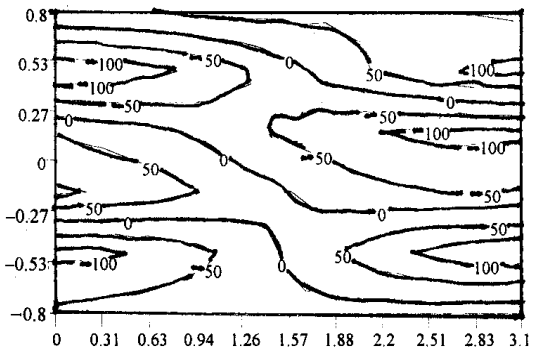

Fig.6 Same as Fig.4 but Pattern III

(3) For Point ③ in Section 3, the atmospheric geopotential of the equilibrium state is shown in Fig.6, being opposite to Fig.4 in general situation. A strong negative anomaly response is present over the equatorial eastern Pacific region and a weak positive anomaly response over the tropical western Pacific and South China Sea. There is a positive anomaly geopotential response in the subtropical area of the eastern Pacific (20°N ~ 30°N) but a large-scale negative anomaly geopotential response in the East Asia subtropical area to the west. It is a situation that is just opposite to the oscillatory phase of east-west and north-south alignment in the atmosphere over the La Niña episode. In addition, the thermal structure of SST during El Niño episode is triggering significant response of negative anomaly geopotential for the subtropical region of East Asia, being unfavorable to the strengthening and northward progression of the subtropical high in the western Pacific summer but favorable for its weakening and persistent southward location.

With the forcing effect of the SST fields of these categories discussed above, the geopotential response of the model atmosphere would have negative anomalous response over warm SST waters and positive anomaly response over cold ones. It agrees well with observed facts and thermal property of the atmosphere. To summarize, the basic features and dynamic processes of the atmospheric response can be concluded as follows:

① The east-west oscillation in the low-latitude areas of the Pacific Ocean is just the opposite to that in the middle- and higher-latitude areas, with the difference in east-west anomaly of the geopotential response from the model atmosphere being the highest and oscillation the most significant within the 10° ~ 15°S and 20° ~ 30°N latitudes. The finding comes close with the latitudinal range of the Southern and Northern Oscillations.

② There are obvious out-of-phase correlation in the north-south direction over the west Pacific of the model domains in Figs.4, 5 and 6, which are similar to the tele-connection pattern found in reality in the region's weather[1, 3]. As indicated in the study by Nitta[7] and Huang et al[8], corresponding to lower (higher) SST in the equatorial east Pacific (west Pacific), convection intensifies around the Philippines and negative anomaly response appears; positive anomaly response appears over East Asia, being favorable for the intensification of the subtropical high; On the contrary, when the SST is getting anomalously warmer (cooler) over the equatorial eastern Pacific (west Pacific), convection near the region of the Philippines would greatly decrease, being favorable for a positive response in the atmospheric geopotential and (maybe) a negative anomaly response over the East Asia region, leading to reduction of the subtropical high in its summer. The experiment results in the current work generally agree with the argument persistent with this research.

③ Patterns similar to the north-south out-of-phase distribution in the western Pacific region are also present in the tropical and subtropical regions of the eastern Pacific. Varying with the positive and negative variation in the SST anomaly in the equatorial east Pacific, they display an oscillatory feature that alternates positively and negatively.

④ The north-south oscillatory response as discussed above can be considered a consequence of propagation along the spherical plane of low-frequency quasi-stationary planetary wavetrains. Due to the important contribution by heating sources in the formation of the quasi-stationary planetary waves, any anomalies in the sources that are corresponding to SST anomaly will eventually produce anomalies in these waves (including the route of wavetrain propagation, positive and negative anomaly and phase, etc), resulting in anomalous and reversed phases in the atmospheric response. It is then an essential mechanism in the north-south oscillatory response of the atmosphere that the conversion of the SST-structured pattern is yielding in-phase or out-of-phase variations of the quasi-stationary planetary wavetrains.

5 RESPONSE FROM ATMOSPHERIC GEOPOTENTIAL FIELD ON SYNOPTIC SCALE

When the horizontal scale $L_0 \sim 10^6$ m and the system are relatively small for the synoptic scale, $A = B = 1.16 \times 10^{-7}$ /s is taken. Corresponding to the pattern of SST distribution discussed above, the response from the atmospheric geopotential field show more of waving or oscillating characteristics.

(1) In the case of Pattern I distribution of the SST field, integration is conducted with the non-linear equation, Eq.(4), for a year (at a time step of 2 h), and results are shown in Fig.7 for corresponding atmospheric geopotential response. With the thermal forcing imposed by the SST field for 1 year, the perturbation of the atmospheric geopotential is of low-frequency oscillation. Fig.8 is an analysis of frequency spectrum that corresponds to the results of numerical integration. It is known from the figure that the frequency spectrum of the oscillation in the atmospheric geopotential perturbation is mainly confined to a frequency range less than 8. Specifically, the first component $q1$ has the maximum value of frequency spectrum of waves at ω = 2 (such large values are also seen at ω = 1), two other secondary maximum values are present at ω = 5, 7, making it oscillating mainly at ω = 2, 1, 5, 7. The third component $q3$ corresponds to significant oscillatory frequencies with large values of frequency spectra at ω = 2, 3, 4, 5 (which have passed a significance test at a confidence level of a = 0.05). The second component has a relatively small oscillatory frequency spectrum $q2$, mainly within the $\omega < 4$ range. Through conversion of time step and duration in the integration, we know that the principal oscillatory periods are approximately 180 and 360 days and the secondary periods are about 72 and 51 days, for the first component; the principle oscillatory periods for the third component are about 180, 120, 90 and 72 days while those of the second component are more than 90 days. In other words, persistent atmospheric heating of SST on the synoptic scale is mainly shown as response patterns oscillating on monthly, seasonal and annual scales. When the SST field is of Type II and III distribution, the numerical integration for the atmospheric geopotential response is similar to the case above. The distributions of frequency spectrum and principal periods are generally consistent with the discussion above.

(2) From the numerical integration results of Fig.7, we also identify such a trend: At the be-

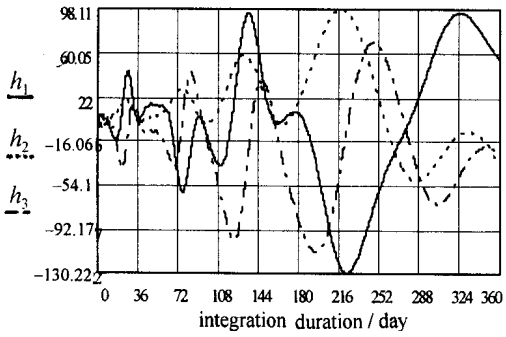

Fig.7 Numerical integration (1 year) of atmospheric geopotential response in association with Pattern I of SST.

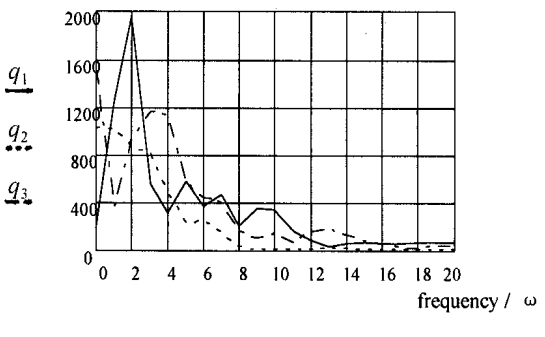

Fig.8 Same as Fig.7 but for its spectral analysis.

ginning of the integration, the atmospheric geopotential response has small amplitudes and short periods, which increase over the length of integration. With the constant thermal forcing of Type I SST field, the response is analyzed for the frequency spectrum over varied periods of integration, as shown in Figs.9 and 10. The figures give a clear picture that individual components of the response have consistent distribution of frequency spectrum. In Fig.9, its main oscillatory frequency is 7 (tested significant with $a = 0.05$), corresponding to an oscillatory frequency of about 13 days (being close to the quasi-biweekly periods of wave in the tropical atmosphere); In Fig.10, the major frequency of oscillation for the atmospheric geopotential response is 4 and the secondary oscillatory frequency is 3 and 5, with corresponding periods of 45 and 60, 36 days in the oscillation (tested significant with $a = 0.05$), comparable with the 30-50 day period in the tropical atmosphere. In Fig.8, the most significant frequency of oscillation concentrates in Domain 1 ~ 4 for the atmospheric geopotential response, corresponding to principle oscillatory periods over 90 days. When the integration is performed over a longer duration (about 500 days later), the response comes to an increasingly stable state of equilibrium (figure omitted). A clear picture can be drawn from comparison of Figs.8, 9 and 10 concerning the magnitude of frequency spectrum and location of major frequencies. It tells that at the early stage, persistent atmospheric thermal forcing of the SST shows itself as perturbations of short periods and mild amplitudes. The amplitude and period increase while the frequency decreases with the continuation of forcing duration, i.e. the response is having a trend of increasing amplitude versus decreasing frequency.

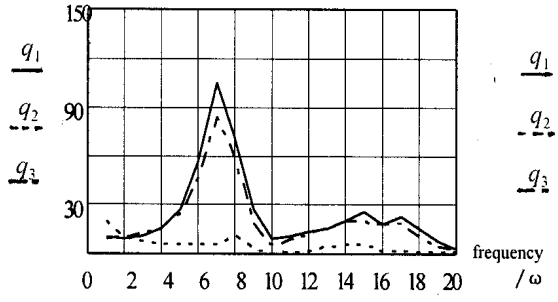

Fig.9 Same as Fig.8 but for integration of 3 months.

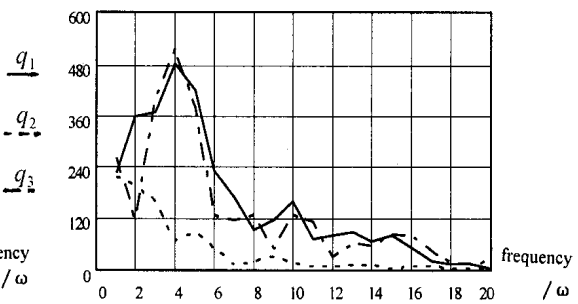

Fig.10 Same as Fig.8 but for integration of 6 months.

It is known from the results above that the SST thermal forcing mainly excites low-frequency atmospheric oscillation at a relatively small synoptic scale. Atmospheric responses with short-lived forcing (less than six months) are mainly associated with quasi-by-weekly waves and 30-50-day oscillation that have short periods while those with long-lived forcing (for up to a year) chiefly give rise to seasonal or annual oscillations with long periods. Such mechanism of wave generation generally reflects on major types of low-frequency waving and oscillation in the tropical atmosphere. As they are popular phenomena in the atmosphere across the global atmosphere, it is inferred that mechanisms for their induction and maintenance are also existing on a stationary basis. The thermal effect of the SST field, which is quite constant, is just the right condition that meets the requirement. It is therefore concluded that the oceanic thermal forcing is playing an essential role in the generation and maintenance of low-frequency oscillation and wave in the tropical atmosphere.

6 CONCLUDING REMARKS

Due to persistent thermal forcing by SST, stable geopotential responses of the atmospheric equilibrium state are excited as main production on the planetary scale. Its mode of response and

pattern are characteristic of oscillations similar to real atmosphere, indicating that the thermal forcing of the ocean and thermal difference are important factors for producing and maintaining the oscillations in the tropical and subtropical regions. Within the synoptic scale, the oceanic thermal forcing mainly produces low-frequency atmospheric oscillation and wave, with long (short) SST thermal forcing exciting long (short) periods in low-frequency oscillations. One of the important features in the process of response is that the response waving is showing the effect of frequency decrease and amplitude increase with the elapse of forcing duration. It is also one of the important channels and physical processes found with the generation of ENSO in the study over recent years.

Acknowledgements: Mr. CAO Chao-xiong, who works at the Guangzhou Institute of Tropical and Oceanic Meteorology, has translated the paper into English.

REFERENCES:

[1] YE Du-zheng, ZENG Qin-cun. Study on Contemporary Climate [M]. Beijing: Meteorological Press, 1991. 8-10, 114-120, 137-152.
[2] SHUKLA J, WALLACE J M. Numerical simulation of the atmospheric response to equatorial Pacific sea surface temperature anomalies [J]. *Journal of Atmospheric Sciences*, 1983, **40**: 1613-1630.
[3] LI Chong-yin. Introduction to Climatic Dynamics [M]. Beijing: Meteorological Press, 1995. 104-109, 144-151, 201-202.
[4] NITTA T. Convective activities in the tropical western Pacific and their impact on the northern hemisphere summer circulation [J]. *Journal of Meteorological Society of Japan*, 1987, **65**: 373-390.
[5] LI Chong-yin, LONG Zhen-xia. Numerical Simulation Study on the Effect of Wintertime Kuroshio Warming on Precipitation during the Raining Season of East China [A]. Research on Issues Related to Climatic Changes [M]. Beijing: Science Press, 1992. 145-156.
[6] LI Chong-yin, The characteristics of the motion in the tropical atmosphere [J]. *Scientia Atmospherica Sinica*, 1985, **9**(4): 366-375.
[7] NITTA T. Long-term variations of cloud amount in the western Pacific region [J]. *Journal of Meteorological Society of Japan*, 1987, **64**: 373-390.
[8] HUANG Rong-hui, LI Wei-jing. The influence of heat source anomalies over the tropical west Pacific in summer on the subtropical high over East Asia and its physical mechanism [J]. *Scientia Atmospherica Sinica*, 1988, (special issue): 107-116.
[9] JI Zhe-rui. Fast Induction to and Application of Mathcad Plus 6.0 [M]. Beijing: Tsinghua University Press, 1998. 115-118.